Received: 17 February 2017 | Accepted: 21 April 2017

DOI: 10.1111/jace.14945

ORIGINAL ARTICLE

Journal of the American Ceramic Society

Enthalpies of formation in the scandia-zirconia system

Robson L. Grosso[1,2] | Eliana N. S. Muccillo[1] | Ricardo H. R. Castro[2]

[1]Center of Science and Technology of Materials, Energy and Nuclear Research Institute, Travessa R 400, Cidade Universitária, Sao Paulo, SP, Brazil

[2]Department of Materials Science and Engineering & NEAT ORU, University of California—Davis, Davis, California

Correspondence
Ricardo H. R. Castro, Department of Materials Science and Engineering & NEAT ORU, University of California—Davis, Davis, CA.
Email: rhrcastro@ucdavis.edu

Funding information
Fundação de Amparo à Pesquisa do Estado de São Paulo, Grant/Award Number: 2014/24022-6; Division of Materials Research, Grant/Award Number: Ceramics 1609781

Abstract

The scandia-zirconia (ScZ) solid solutions have been attracting attention from the communities interested in solid-oxide fuel cells because they possess the highest ionic conductivity among zirconia-based materials. However, this system shows a relatively large number of polymorphs with lack of thermodynamic data to enable comprehensive phase control for property optimization. In this work, the enthalpy of formation of the ScZ system within the range 0–20 mol% Sc_2O_3 is determined by combining the surface energy values with enthalpy of drop solution data obtained from high-temperature oxide melt solution calorimetry. The heats of formation, a key data for understanding phase stability, for five polymorphs: monoclinic (*m*), tetragonal (*t*), cubic (*c*), and rhombohedral (β and γ) are reported for the first time.

KEYWORDS

phase diagrams, scandium/scandium compounds, Thermodynamics, Zirconia

1 | INTRODUCTION

Although yttria-stabilized zirconia (YSZ) is the most studied material for solid electrolyte application in solid oxide fuel cell (SOFC), alternative doping of zirconia with scandia promotes higher ionic conductivity values in cubic fluorite-structured ZrO_2.[1] Thus, the scandia-zirconia (ScZ) system has been recognized as a promising electrolyte candidate for the next-generation SOFC, operating at intermediate temperatures (650-850°C).[1-3]

Nevertheless, the phase stability of the ScZ is considered complex and data on heat of formation to enable phase prediction are scarce. Several phases have been reported for this system as a function of scandia content: monoclinic (*m*), tetragonal (*t*), cubic (*c*), and three ordered rhombohedral structures (β, γ, δ).[1,4] Two tetragonal phases (*t*' and *t*'') have been also identified.[4-6] According to the phase diagram,[4] compositions with low Sc_2O_3 content (<4 mol%) show monoclinic phase. The tetragonal stability range is reported from 4 to 8 mol%. Rhombohedral β phase is stabilized in compositions between 8 and 12 mol% Sc_2O_3 at room temperature. The highest ionic conductivity is, however, found for cubic fluorite structure, which is only achieved at high temperatures (close to 600°C) also in the 8–12 mol% range due to the β-*c* reversible phase transition.[7] Even when the cubic phase is obtained, a degradation of its ionic conductivity occurs in SOFC operating conditions due to the spontaneous phase transitions.[7-9]

The cubic fluorite phase stabilization and long-term stability have been the focus of several researches in the past years.[1,7-10] According to literature, the precipitation of secondary phases as function of time is a detrimental factor for ionic conductivity. Whereas the formation of tetragonal phases in cubic matrix takes place for compositions lower than 10 mol% Sc_2O_3,[1,7-9] rhombohedral phase precipitation usually occurs above 10 mol%.[7-10] Thereby, this combination of difficulty of cubic phase stabilization and degradation of the ionic conductivity prevent ScZ system application as a commercial solid electrolyte.

Recent studies have shown that cubic phase stabilization of ScZ can be achieved by introducing a second additive[9,11,12] or by decreasing the grain size to the nanoscale.[6,13-15] The grain size effect on polymorphism of oxides has been extensively studied in the literature and relates to the role of surface energies in the total energy of the system.[16,17] For instance, because of its symmetry,

cubic polymorphs tend to have lower surface energies, allowing an increased thermodynamic stability (related to other polymorphs with higher surface energies) when the particle sizes are small.[14,18,19] In fact, the grain size dependence on the stability of polymorphs allows obtaining particles with crystalline structures that are otherwise unstable in the bulk form. The relative easy access to those phases can thus enable a complete thermodynamic analysis for building reliable and complete bulk phase diagrams.

However, from a thermodynamic perspective, although one can stabilize several polymorphs at the nanoscale, the energetic contribution from surface and bulk crystal needs to be separated if the goal is to construct an actual bulk phase diagram, i.e., without surface contributions. Due to recent advances in microcalorimetry,[20-22] reliable surface energy data for the five polymorphs of the ScZ system: monoclinic, tetragonal, cubic, rhombohedral β, and γ have been reported recently.[14] In this work, we combined the surface energy values with enthalpy of drop solution data obtained from high-temperature oxide melt solution calorimetry experiments to determine the bulk enthalpy of drop solution (ΔH_{DS}) of ScZ within the compositional range 0-20 mol% Sc_2O_3, whose formula can be written as $Sc_xZr_{1-x}O_{2-x/2}$ ($0.022 \leq x \leq 0.324$). With this, the enthalpies of formation at room temperature ($\Delta H_{f,ox}$) of the five ScZ polymorphs were reported, enabling future phase diagram elaborations.

2 | EXPERIMENTAL PROCEDURE

2.1 | Preparation

Nanopowders of scandia-zirconia ($Sc_xZr_{1-x}O_{2-x/2}$) with 0-20 mol% Sc_2O_3 ($0.022 \leq x \leq 0.324$) were synthesized by reverse-strike coprecipitation method. Starting solutions of scandium nitrate hydrate (99.9%, Alfa Aesar, Ward Hill, MA) and zirconyl nitrate hydrate (99%, Sigma-Aldrich, St. Louis, MO) were prepared by dissolution in deionized water to form a clear dilute solution. The cation concentration was verified by gravimetry. Stoichiometric amounts of the starting solutions were mixed together and concentration was adjusted to 0.5 M. The resultant solution was dropped point-wise into a magnetically stirred 5 M excess ammonium hydroxide solution until complete precipitation. The gelatinous precipitated was washed and centrifuged three times using water, ethanol (50%), and denatured ethanol to remove any residual ammonium on the precipitated hydroxide. The powder was subsequently dried at 100°C for 48 hours and grounded in an agate mortar. The dried hydroxide powders were calcined in a box furnace within a wide range of temperatures 450-1500°C (high-temperature range used to produce reference coarsened samples). Details of grain size and crystalline structure encountered for each evaluated calcination condition were reported previously.[14]

2.2 | Characterization

Crystalline phases present on the calcined scandia-zirconia powders were analyzed by X-ray diffraction (XRD) using a Bruker-AXS (Billerica, MA) D8 Advance diffractometer operated with Cu$K\alpha$ radiation (λ=1.5405 Å). Data were acquired over a range of 2θ between 20 and 90° with a step size of 0.01° and a collection time of 0.4 s/step. Phase identification, lattice parameters, and grain sizes were determined using JADE 6.1 software to perform a whole profile fitting (WPF) refinement. PDF#51-1602 for monoclinic (*m*), PDF#51-1603 for tetragonal (*t*), PDF#64-9607 for cubic (*c*), PDF#64-9610 rhombohedral β, and PDF#61-7752 rhombohedral γ were used for refinements. Silicon standard was mixed to ScZ powders in order to ensure accuracy in lattice parameter determination. PDF#27-1402 was used for silicon standard refinement.

The chemical composition of all synthesized samples was measured by wavelength-dispersive X-ray spectroscopy (WDS) electron probe microanalysis using a Cameca SX100 (Gennevilliers, France) microprobe at accelerating voltage of 15 kV, 10 nA beam current, and 5 μm beam size. An average of 10 data points was used to calculate sample composition. Uncertainties in chemical composition were lower than 5%.

For determination of the enthalpies of formation of $Sc_xZr_{1-x}O_{2-x/2}$ ($0.022 \leq x \leq 0.324$) solid solutions, high-temperature oxide melt drop solution calorimetry was performed at 700°C using a custom-built Tian-Calvet (Davis, CA) calorimeter.[23] Approximately 5 mg of nano and bulk samples were lightly pressed into pellets, weighted, and dropped from room temperature into $3Na_2O.4MoO_3$ melted solvent at 700°C. During the experiments, oxygen flushing (40 mL/min) and bubbling (3.5 mL/min) were applied to ensure that the final oxygen state was constant and to further sample dissolution. Calorimeter calibration was performed using the heat content of α-Al_2O_3 pellets of similar weight. Prior to the experiments, all samples were equilibrated in a 50% relative humidity environment for 72 hours to establish a constant water content, which was quantified by thermogravimetric experiments. At least eight drops of sample were performed in order to get statistically meaningful data. The heats of dissolution were treated with thermochemical cycles, in particular to address the water desorption/evaporation energies, as reported elsewhere.[14] That is, the heat of dissolution of nanoparticles is a combination of bulk and surface dissolution, along with water desorption and evaporation, following the cycle (Table 1). Heat effects related to water can be quantified by using water adsorption microcalorimetry and has been previously reported by the authors for the ScZ polymorphs studied here.[14]

TABLE 1 Thermochemical cycle used for correction of $Sc_xZr_{1-x}O_{2-x/2}$ enthalpy of drop solution at 700°C (ΔH_{DS})

$ScZ_{(nano,\ 25°C)}{\cdot}yH_2O_{(adsorbed,\ 25°C)} \rightarrow ScZ_{(dissolved,\ 700°C)}+yH_2O_{(g,\ 700°C)}$	ΔH_{DS}
$yH_2O_{(l,\ 25°C)} \rightarrow yH_2O_{(g,\ 700°C)}$	$\Delta H_w = y(25.0\pm0.1)$ kJ/mol
$yH_2O_{(adsorbed,\ 25°C)} \rightarrow yH_2O_{(l,\ 25°C)}$	$-y\Delta H_{adsorption}$
$ScZ_{(nano,\ 25°C)} \rightarrow ScZ_{(bulk,\ 25°C)}$	$-SE.SA$
$ScZ_{(bulk,\ 25°C)} \rightarrow ScZ_{(dissolved,\ 700°C)}$	ΔH_{bulk}
$\Delta H_{DS}=\Delta H_w - y\Delta H_{adsorption} - SE.SA+\Delta H_{bulk}$	

y = total water content determined by thermogravimetry; SE = surface energy; SA = surface area.

3 | RESULTS AND DISCUSSION

Several calcination conditions, varying temperature and dwell time, were evaluated in order to obtain single-phase samples in the studied composition range of ScZ. All investigated compositions and crystalline phases identified for each sample are listed in Table 2. The samples were crystalline and showed a single phase as determined from XRD analysis.[14] The scandia concentrations are indicated as Sc_2O_3, $ScO_{1.5}$, and x to facilitate comprehension. Five polymorphs (monoclinic, tetragonal, cubic, rhombohedral β, and γ) of $Sc_xZr_{1-x}O_{2-x/2}$ ($0.022 \le x \le 0.324$) were evaluated.

The lattice parameter for $Sc_xZr_{1-x}O_{2-x/2}$ fluorite cubic samples with x varying between 0.155 and 0.324 is presented in Figure 1. Decrease in the lattice parameter with increasing Sc content is observed, in agreement with independent reports.[24] This behavior is typical of solid solutions formed by addition of smaller cations.[25] However, the ionic radius of Sc^{3+} (0.87 Å)[26] is slightly higher than Zr^{4+} (0.84 Å)[26] in eightfold coordination. Considering only ionic radius, lattice parameter is expected to be larger by increasing Sc content, as observed in ZrO_2-containing Y^{3+} (1.019 Å) and Yb^{3+} (0.985 Å) solid solutions.[27,28]

The behavior encountered in the ScZ system may be associated with structural shrinkage due to increasing oxygen vacancy concentration causing distortions of cations and anions sublattices and consequently decreasing lattice parameter. Although Y^{3+} and Yb^{3+} additions also produce oxygen vacancies in fluorite ZrO_2, the opposite effect of ScZ system in terms of lattice parameter can be attributed to significant smaller mismatch between Sc^{3+} and Zr^{4+} ionic radius. In agreement with this picture, based on classical molecular dynamics simulation,[29] the average coordination number of both Sc^{3+} and Zr^{4+} tends to decrease with increase in the Sc^{3+} content leading to smaller lattice parameters. These results are consistent with the chemical expansion coefficient model for related fluorite-structured materials, where the lattice contraction/expansion is

TABLE 2 Enthalpy of drop solution (ΔH_{DS}) and enthalpy of formation ($\Delta H_{f,ox}$) of $Sc_xZr_{1-x}O_{2-x/2}$ ($0.022 \le x \le 0.324$) obtained for five polymorphs

Sc_2O_3 (mol%)	$ScO_{1.5}$ (mol%)	x	ΔH_{DS} (kJ/mol)[a]	$\Delta H_{f,ox}$ (kJ/mol)
Monoclinic				
1.1	2.2	0.022	16.9±1.3	1.54±1.4
2.1	4.1	0.041	6.7±0.7	10.8±0.9
Tetragonal				
1.1	2.2	0.022	−6.6±1.3	25.0±1.4
2.1	4.1	0.041	−11.6±1.5	29.1±1.6
3.1	6	0.060	−14.9±2.0	31.5±2.0
4.2	8.1	0.081	−7.5±2.1	23.1±2.2
6.3	11.9	0.119	−3.3±1.2	17.0±1.5
Cubic				
8.4	15.5	0.155	−8.3±0.3	20.3±1.0
10.6	19.2	0.192	−16.1±1.8	26.3±2.0
11.6	20.8	0.208	−14.1±2.2	23.5±2.2
12.9	22.9	0.229	−23.5±1.2	31.9±1.4
13.6	23.9	0.239	−21.1±1.5	29.0±1.6
19.3	32.4	0.324	−31.8±2.0	35.6±2.1
Rhombohedral β				
10.6	19.2	0.192	−2.3±1.2	12.5±1.5
11.6	20.8	0.208	2.0±2.5	7.43±2.5
12.9	22.9	0.229	−3.9±0.2	12.3±0.7
Rhombohedral γ				
13.6	23.9	0.239	−2.5±1.0	10.4±1.1
14.3	25	0.250	−4.3±2.5	11.7±2.7
19.3	32.4	0.324	−7.7±1.0	11.5±1.2

[a]Solvent: molten $3Na_2O.4MoO_3$ at 700°C.

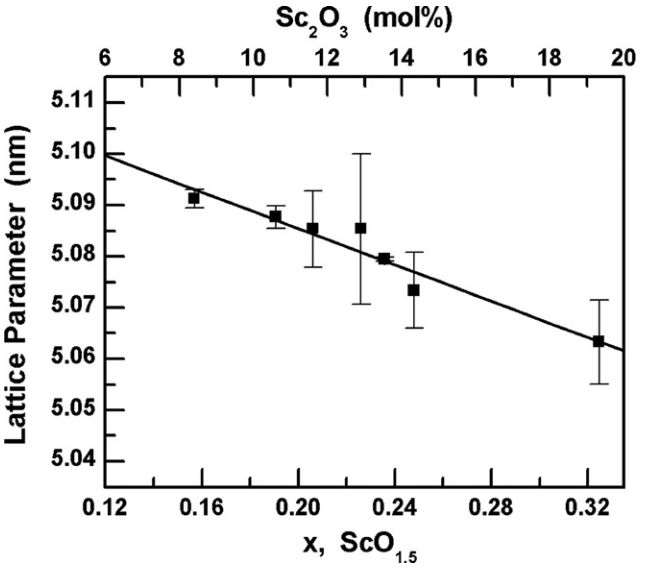

FIGURE 1 Lattice parameter of cubic $Sc_xZr_{1-x}O_{2-x/2}$ solid solution as a function of scandia content

TABLE 3 Thermochemical cycle used for calculation of $Sc_xZr_{1-x}O_{2-x/2}$ (bulk) enthalpy of formation at 25°C ($\Delta H_{f,ox}$)

$ZrO_{2(monoclinic,\ 25°C)} \rightarrow ZrO_{2(dissolved,\ 700°C)}$	$\Delta H_{DS}(ZrO_2)$[a]
$ScO_{1.5(C\text{–}type,\ 25°C)} \rightarrow ScO_{1.5(dissolved,\ 700°C)}$	$\Delta H_{DS}(ScO_{1.5})$[b]
$Sc_xZr_{1-x}O_{2-x/2(s,\ 25°C)} \rightarrow x ScO_{1.5(dissolved,\ 700°C)} + (1-x)ZrO_{2(dissolved,\ 700°C)}$	$\Delta H_{DS}(x\text{ScZ})$
$ScO_{1.5(C\text{–}type,\ 25°C)} + ZrO_{2(monoclinic,\ 25°C)} \rightarrow Sc_xZr_{1-x}O_{2-x/2(s,\ 25°C)}$	$\Delta H_{f,ox}(x\text{ScZ})$
$\Delta H_{f,ox}(x\text{ScZ}) = x\Delta H_{DS}(ScO_{1.5}) + (1-x)\Delta H_{DS}(ZrO_2) - \Delta H_{DS}(x\text{ScZ})$	

[a] 19.5±0.3 kJ/mol.[14,31]
[b] −28.9±0.4 kJ/mol.[31,32]

governed by two competing processes: formation of a vacancy (leading to a lattice contraction) and the cation radius change (leading to a lattice expansion).[30]

Table 2 lists the enthalpies of drop solution at 700°C (ΔH_{DS}) and the enthalpies of formation at 25°C ($\Delta H_{f,ox}$) obtained for all investigated samples. The enthalpies of formation were calculated from the drop solution data via a thermochemical cycle presented in Table 3. The enthalpies of drop solution of monoclinic ZrO_2 and C-type cubic bixbyite $ScO_{1.5}$ used in this study were 19.5±0.3[14,31] and −28.9±0.4 kJ/mol,[31,32] respectively.

The enthalpies of formation of the five investigated polymorphs of ScZ were plotted as a function of scandia content (Figure 2). For low Sc_2O_3 contents (<4 mol%), the more exothermic enthalpies of formation indicate that

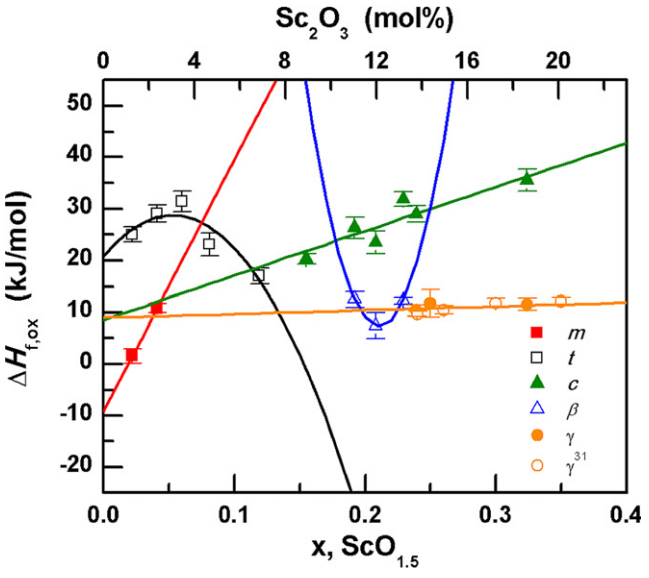

FIGURE 2 Enthalpies of formation for five polymorphs (*m*=monoclinic, *t*=tetragonal, *c*=cubic, rhombohedral β and γ phases) of $Sc_xZr_{1-x}O_{2-x/2}$ as a function of scandia content [Color figure can be viewed at wileyonlinelibrary.com]

monoclinic polymorph is the most thermodynamically stable phase at room temperature, in agreement with independent reports.[6,10,14,24] The values become less exothermic with increasing Sc^{3+} concentration favoring tetragonal transformation.

Similar values were encountered for tetragonal and cubic polymorphs around 6-8 mol% Sc_2O_3. The proximity of the $\Delta H_{f,ox}$ for *t* and *c* polymorphs suggests that *t*-*c* phase transition is thermodynamically favorable, explaining the easiness of formation of tetragonal phases in the cubic matrix reported in the literature.[1,6-9,15] This formation of tetragonal phases (*t*, *t*', and *t*'') in a cubic matrix is an undesirable event, occurring for unclear reasons until now, that is responsible for an observed decrease in ionic conductivity observed for compositions between 7 and 10 mol % Sc_2O_3 during aging at temperatures ≥600°C.

The more exothermic enthalpies found for rhombohedral phases indicate the stability of these structures at room temperature. The data agree with the stability trend of β and γ phases in bulk samples for compositions higher than 10 mol% Sc_2O_3.[1,4,14,24,33] In addition, the enthalpies of formation of rhombohedral (γ) ScZ samples agree very well with reported data[31] and are consistent with the phase diagram previously suggested for ScZ.[14]

According to literature, enthalpies of formation should become less exothermic with decreasing dopant ionic radius in fluorite-zirconia-based materials.[31,34] However, ScZ cubic phases shows an inverse function, as plotted in Figure 3. Figure 3 shows $\Delta H_{f,ox}$ of ScZ and YZ cubic fluorite solid solutions as a function of additive (M=Sc and Y) content. While for YZ the curve can be clearly represented by a quadratic fitting function with initial negative slopes, in the studied composition range, ScZ can be well fitted by both linear or quadratic equations with initial positive slopes. Note that although both linear or quadratic equations do fit, a reference[31] reporting enthalpies of formation of rare earth-, yttrium-, and scandium-stabilized zirconia and hafnia showed better fitting with a quadratic function to extract interaction parameters and enthalpies of transition, which suggesting a similar fitting should be adopted here.

Analyzing the curve, the initial point (*x*=0) corresponds to the transformation enthalpy of ZrO_2 from monoclinic to cubic fluorite structure ($\Delta H_{m\rightarrow c}$=8.8±3.4 kJ/mol).[31,34] For increasing dopant contents, the formation enthalpies of cubic ScZ are endothermic, in contrast to those of YZ which are exothermic. According to Simoncic and Navrotsky,[31] these results indicate the smallest extent of short range order of ScZ system which is associated with similar ionic radii of Zr^{4+} and Sc^{3+}. The strong short range order declines ionic conductivity by decreasing the mobility of oxygen vacancies.[31,34] Thereby, among cubic fluorite solid solutions, the endothermic enthalpies of formation of ScZ

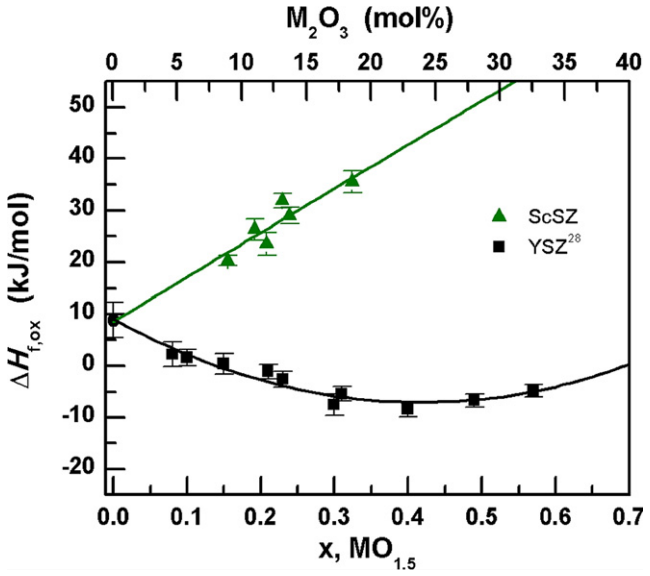

FIGURE 3 Enthalpies of formation of cubic fluorite $M_xZr_{1-x}O_{2-x/2}$ (M=Sc and Y) solid solutions (ScSZ=scandia-stabilized zirconia; YSZ=yttria-stabilized zirconia) [Color figure can be viewed at wileyonlinelibrary.com]

suggest less ordering, consistent to the highest ionic conductivity values.[1,3] On the other hand, the endothermic enthalpy of formation confirms the experimental difficulty in obtaining the cubic polymorph is rooted on a thermodynamic property.

4 | CONCLUSIONS

The enthalpies of formation for the five polymorphs (monoclinic, tetragonal, cubic, rhombohedral β, and γ) of the scandia-zirconia system were determined by combining surface energy values with enthalpy of drop solution data obtained from high-temperature oxide melt solution calorimetry. Spontaneous phase transitions in ScZ solid solutions are explained based on the enthalpy of formation data. The complete set of data provides the possibility for more accurate composition and processing design for obtaining optimal ScZ cubic phase.

ACKNOWLEDGMENT

The authors would like to thank Nick Botto for performing the electron microprobe analysis. This work was financially supported by the FAPESP (2014/24022-6) and National Science Foundation DMR Ceramics 1055504 and 1609781.

REFERENCES

1. Badwal SPS, Ciacchi FT. Oxygen-ion conducting electrolyte materials for solid oxide fuel cells. *Ionics*. 2000;6:1-21.
2. Lashtabeg A, Skinner SJ. Solid oxide fuel cells - a challenge for materials chemists? *J Mater Chem*. 2006;16:3161-3170.
3. Gao Z, Mogni LV, Miller EC, Railsback JG, Barnett SA. A perspective on low-temperature solid oxide fuel cells. *Energy Environ Sci*. 2016;9:1602-1644.
4. Ruh R, Garrett HJ, Domagala RF, Patel VA. The system zirconia-scandia. *J Am Ceram Soc*. 1977;60:399-403.
5. Abdala PM, Lamas DG, Fantini MCA, Craievich AF. Retention at room temperature of the tetragonal t″-form in Sc_2O_3-doped ZrO_2 nanopowders. *J Alloys Compd*. 2010;495:561-564.
6. Xu G, Zhang YW, Liao CS, Yan CH. Doping and grain size effects in nanocrystalline ZrO_2-Sc_2O_3 system with complex phase transitions: XRD and Raman studies. *Phys Chem Chem Phys*. 2004;6:5410-5418.
7. Badwal S. Scandia-zirconia electrolytes for intermediate temperature solid oxide fuel cell operation. *Solid State Ionics*. 2000;136–137:91-99.
8. Araki W, Koshikawa T, Yamaji A, Adachi T. Degradation mechanism of scandia-stabilised zirconia electrolytes: discussion based on annealing effects on mechanical strength, ionic conductivity, and Raman spectrum. *Solid State Ionics*. 2009;180:1484-1489.
9. Haering C, Roosen A, Schichl H, Schnöller M. Degradation of the electrical conductivity in stabilised zirconia system Part II: scandia-stabilised zirconia. *Solid State Ionics*. 2005;176:261-268.
10. Badwal SPS. Effect of dopant concentration on electrical conductivity in the Sc_2O_3-ZrO_2 system. *J Mater Sci*. 1987;22:4125-4132.
11. Grosso RL, Tertuliano AJ, Machado IF, Muccillo ENS. Structural and electrical properties of spark plasma sintered scandia- and dysprosia-stabilized zirconia. *Solid State Ionics*. 2016;288:94-97.
12. Tietz F. Structural evolution of Sc-containing zirconia electrolytes. *Solid State Ionics*. 1997;100:289-295.
13. Okamoto M, Akimune Y, Furuya K, Hatano M, Yamanaka M, Uchiyama M. Phase transition and electrical conductivity of scandia-stabilized zirconia prepared by spark plasma sintering process. *Solid State Ionics*. 2005;176:675-680.
14. Grosso RL, Muccillo ENS, Castro RHR. Phase stability in scandia-zirconia nanocrystals. *J Am Ceram Soc*. 2017;100:2199-2208.
15. Abdala PM, Fantini MCA, Craievich AF, Lamas DG. Crystallite size-dependent phases in nanocrystalline ZrO_2-Sc_2O_3. *Phys Chem Chem Phys*. 2010;12:2822-2829.
16. Garvie RC. The occurrence of metastable tetragonal zirconia as a crystallite size effect. *J Phys Chem*. 1965;69:1238-1243.
17. Gouvea D, Castro RHR. Sintering and nanostability: the thermodynamic perspective. *J Am Ceram Soc*. 2016;99:1105-1121.
18. Drazin JW, Castro RHR. Phase stability in nanocrystals: a predictive diagram for yttria-zirconia. *J Am Ceram Soc*. 2015;98:1377-1384.
19. Drazin JW, Castro RHR. Phase stability in calcia-doped zirconia nanocrystals. *J Am Ceram Soc*. 2016;99:1778-1785.
20. Ushakov SV, Navrotsky A. Direct measurements of water adsorption enthalpy on hafnia and zirconia surface using novel design for gas adsorption microcalorimetry. *Appl Phys Lett*. 2005;87:164103.
21. Castro RHR, Quach DV. Analysis of anhydrous and hydrated surface energies of gamma-Al_2O_3 by water adsorption microcalorimetry. *J Phys Chem C*. 2012;116:24726-24733.
22. Drazin JW, Castro RHR. Water adsorption microcalorimetry model: deciphering surface energies and water chemical potentials

of nanocrystalline oxides. *J Phys Chem C*. 2014;118:10131-10142.

23. Navrotsky A. Progress and new directions in high temperature calorimetry. *Phys Chem Miner*. 1977;2:89-104.
24. Fujimori H, Yashima M, Kakihana M, Yoshimura M. Structural changes of scandia-doped zirconia solid solutions: Rietveld analysis and Raman scattering. *J Am Ceram Soc*. 1998;81:2885-2893.
25. Bulavchenko OA, Vinokurov ZS, Afonasenko TN, et al. Reduction of mixed Mn-Zr oxides: in situ XPS and XRD studies. *Dalt Trans*. 2015;44:15499-15507.
26. Shannon RD. Revised effective ionic radii and systematic studies of interatomic distances in halides and chalcogenides. *Acta Crystallogr Sect A*. 1976;32:751-767.
27. Strickler DW, Carlson WG. Electrical conductivity in the ZrO_2-rich region of several M_2O_3-ZrO_2 systems. *J Am Ceram Soc*. 1965;48:286-289.
28. Lee TA, Navrotsky A, Molodetsky I. Enthalpy of formation of cubic yttria-stabilized zirconia. *J Mater Res*. 2003;18:908-918.
29. Devanathan R, Thevuthasan S, Gale JD. Defect interactions and ionic transport in scandia stabilized zirconia. *Phys Chem Chem Phys*. 2009;11:5506-5511.
30. Marrocchelli D, Bishop SR, Tuller HL, Yildiz B. Understanding chemical expansion in non-stoichiometric oxides: ceria and zirconia case studies. *Adv Funct Mater*. 2012;22:1958-1965.
31. Simoncic P, Navrotsky A. Systematics of phase transition and mixing energetics in rare earth, yttrium, and scandium stabilized zirconia and hafnia. *J Am Ceram Soc*. 2007;90:2143-2150.
32. Cheng J, Navrotsky A. Enthalpies of formation of $LaBO_3$ perovskites (B = Al, Ga, Sc, and In). *J Mater Res*. 2003;18:2501-2508.
33. Yao L, Liu W, Ou G, Nishijima H, Pan W. Phase stability and high conductivity of ScSZ nanofibers: effect of the crystallite size. *J Mater Chem A*. 2015;3:10795-10800.
34. Navrotsky A. Thermodynamics of solid electrolytes and related oxide ceramics based on the fluorite structure. *J Mater Chem*. 2010;20:10577-10587.

How to cite this article: Grosso RL, Muccillo ENS, Castro RHR. Enthalpies of formation in the scandia-zirconia system. *J Am Ceram Soc*. 2017;100:4270–4275. https://doi.org/10.1111/jace.14945